Feasibility study of nicotine identification and adsorption by $B_{12}N_{12}$ nanostructure using computational methods.

Sepehr Barzgar, Aydin Bahrami

Abstract:

The first-principle calculations employing density functional theory (DFT) at the M062X/6-311++G** level were utilized to the examine the adsorption tendencies of nicotine molecules on the other surface of pristine $B_{12}N_{12}$ nano-cages. To understand the binding characteristics between the $B_{12}N_{12}$ complex as adsorbent and nicotine, the structural and electronic parameters, including Natural Bond Orbital (NBO) and Atoms in Molecules (AIM) properties were analyzed. The results indicate that nicotine tends to adsorb preferentially via its nitrogen atom, situated on 6-membered BN ring onto the Lewis acid sites of B atoms within the nano-cages. Based on the calculated density of states, the interaction between nicotine and the external wall of $B_{12}N_{12}$ results in significant variations in their conductivities, thereby suggesting its potential suitability as a nicotine sensor. Presence of polar solvent enhances the adsorption of nicotine onto the nano-cage. Furthermore, AIM-based analyses suggested an electrostatic nature for N-B interaction within the Nicotine…$B_{12}N_{12}$ complex. According to the calculated results, the $B_{12}N_{12}$ nano-cage shows promise as an effective absorbent and sensor for detecting nicotine in environmental systems.

Keywords: Adsorption, Nicotine, $B_{12}N_{12}$ nano-cages, Sensor, Density functional theory.

Introduction:

Nicotine, a naturally occurring alkaloid found in tobacco plants, possesses both benefits and drawbacks. On the positive side, nicotine has been linked to several cognitive and physiological effects.[1] It acts as a stimulant, increasing alertness, concentration, and cognitive function in some individuals. Additionally, nicotine has been associated with mood enhancement and stress reduction, leading some people to use it as a form of self-medication for anxiety or depression. However, nicotine also carries significant health risks and addictive properties.[2] Prolonged use of nicotine, particularly through smoking tobacco products, is a leading cause of preventable death worldwide. Nicotine addiction can result in physical dependence, making it challenging for individuals to quit despite the associated health risks.[3] Furthermore, nicotine consumption is linked to numerous adverse health effects, including increased heart rate and blood pressure, respiratory issues, and an increased risk of cardiovascular diseases and certain cancers.[4]

Despite its risks, nicotine has been studied for its potential therapeutic applications. Nicotine replacement therapies, such as nicotine patches and gums, are used to help individuals quit smoking by gradually reducing nicotine dependence.[5] Additionally, research is ongoing to explore nicotine's potential in treating neurological disorders such as Parkinson's disease and Alzheimer's disease.[6]

Boron nitride nanocages, with their unique structure and properties, have garnered significant attention in the field of nanotechnology. These nanocages, composed of $B_{12}N12$ units, exhibit remarkable stability, high surface area, and excellent thermal and chemical resistance.[7] They hold promise for various applications, including gas storage, drug delivery, catalysis, and nanoelectronics. The precisely engineered pores and cavities within these nanocages enable efficient encapsulation of guest molecules, making them ideal candidates for targeted drug delivery systems.[8] Moreover, their thermal stability and chemical inertness make them suitable for harsh

industrial environments. Research into boron nitride nanocages continues to uncover their potential across a wide range of fields, highlighting their importance in advancing nanotechnology and materials science.[9]

Nano cages are nanostructures with hollow interiors that can encapsulate guest molecules. They are typically composed of various materials, including carbon, metal oxides, and metal organic frameworks. Nano cages exhibit unique properties due to their nanoscale size and porous structure.[10]

One of the key characteristics of nano cages is their high surface area-to-volume ratio, which allows for efficient adsorption and storage of guest molecules. This property makes them promising candidates for applications such as gas storage, drug delivery, and catalysis.[11]

Additionally, nano cages can be precisely engineered to control the size and shape of their pores, enabling selective adsorption of molecules based on their size, shape, and polarity. This tunability makes nano cages versatile platforms for designing advanced materials with tailored properties.[12]

Furthermore, nano cages often exhibit excellent stability, mechanical strength, and chemical resistance, making them suitable for use in harsh environments and demanding applications.[13]

Overall, nano cages hold significant potential for a wide range of scientific and technological applications, thanks to their unique structural and functional properties. Ongoing research in this field continues to uncover new ways to harness the capabilities of nano cages for various industrial and biomedical applications.[14]

The aim of this research is to use first-principles computations to analyze how Nicotine molecules interact with the external surface of pristine $B_{12}N_{12}$ nano-cages. By utilizing computational calculations, we can determine the effectiveness of using a new substance as an

adsorbent for specific analytes or compounds without the need for costly and time-consuming experimental tests in the laboratory.[15] This approach not only reduces the overall cost of analysis by eliminating trial and error experiments but also provides a deeper understanding of the underlying mechanisms involved in the adsorption process.

The use of first-principles computations in this study allows us to make predictions about the potential adsorption behavior of nicotine molecules on the external surface of $B_{12}N_{12}$ nano-cages. By analyzing the interactions between the nicotine molecule and the nano-cage, we can assess whether this particular system would be a suitable adsorbent for a given analyte or class of compounds.[16] This predictive capability is especially valuable in the field of adsorption studies, where the ability to quickly evaluate the efficiency of an adsorbent can streamline the research process and lead to more targeted experimental investigations.[17]

Furthermore, the insights gained from computational calculations can also enhance our understanding of the underlying mechanisms driving the adsorption process. By studying the interactions at the molecular level, we can identify key factors that influence the adsorption behavior of the nicotine molecule on the nano-cage surface. This knowledge can then be used to optimize the adsorption process and potentially improve the performance of the adsorbent material.[18]

Overall, the use of first-principles computations in this study offers a valuable tool for predicting the adsorption behavior of nicotine molecules on $B_{12}N_{12}$ nano-cages. By leveraging computational calculations, researchers can efficiently assess the suitability of new adsorbent materials without the need for extensive experimental testing. This approach not only saves time and resources but also provides a deeper understanding of the adsorption mechanisms at play, ultimately leading to more effective adsorption processes in the future.[19]

Computational methods

DFT Calculations:

The Gaussians software package facilitated electronic structure calculations. Geometrical parameters for pristine $B_{12}N_{12}$ were fully optimized using the M062X functional and the 6-311++G** basis set to achieve the most stable complexes.[20] Two types of active sites on the exterior surface of $B_{12}N_{12}$ were investigated, considering all possible orientations for nicotine as a ligand. Frequency calculations at the M06/6-311++G** level confirmed the optimized geometries as minima on the potential energy surface.[21] Binding energies were adjusted for basis set superposition errors (BSSE) using the counterpoise method. Results indicated one complex structure to be thermodynamically more stable, aligning with expectations of Lewis acid-base interactions. Group V atoms like nitrogen, being electron-rich, form strong covalent bonds with surface B atoms.[22]

The adsorption energy (E_{ad}) of NIC is calculated as:

$E_{ad} = E_{tot}$ ($B_{12}N_{12}$/Nicotine) - E_{tot} ($B_{12}N_{12}$) - E_{tot} (Nicotine),

where negative values denote exothermic adsorption. Solvation effects (water) were examined using the polarized continuum model (PCM).[23] Electron Density of States (DOSs) were generated using Gauss Sum, and the sensitivity of $B_{12}N_{12}$ complexes in terms of the HOMO–LUMO gap (E_g) was compared during the adsorption process. In DOS graphs, E_g signifies the energy gap between the valence (HOMO) and conduction (LUMO) levels in insulators and semiconductors.[24]

Atoms in Molecules (AIM) calculations:

To examine the electron density and bonding properties of the systems under investigation, we employed the AIM methodology.[25] Bond critical points (BCPs) were identified to extract the

charge density and the Laplacian of the charge density at each point, facilitating discussion on the interaction nature.[26] AIM analyses were conducted using the AIM 2000 package at the M062X/6-311++G** level of theory.[27]

Results and discussion:

Analysis of binding energies and structural parameters:

Figure 1 depicts the optimized structure of the $B_{12}N_{12}$ nano-cage alongside its DOS plot, revealing the nano-cage as an insulator with a HOMO–LUMO gap (E_g) of 9.34 eV. Determination of stable configurations for single nicotine adsorbed on the nano-cage was guided by the molecular electrostatic potential (MEP) plot of single nicotine, illustrated in Figure 2. The figure highlights the partial negative charge on the N atom of the hexagon ring of nicotine as a reactive site for Lewis acid interactions with B atoms, allowing nicotine molecules to approach the external surface of the $B_{12}N_{12}$ nano-cage. Additionally, the H atoms of the 5-membered ring of NIC exhibit a favorable trend as reactive sites for base acid interactions with N atoms on the external surface of $B_{12}N_{12}$. Two stable structures for nicotine adsorption on the nano-cage, presented in Figure 3, are categorized into physisorption and chemisorption. The former is attributed to strong interaction of the N atom with the $B_{12}N_{12}$ nano-cage, while the latter involves weak interaction of nicotine with the nano-cage through van der Waals forces. In the chemisorption configuration, the distance between N and B atoms, as well as E_b and E_g values, are determined as 1.61 Å, -37.38 kcal/mol, and 6.84 eV, respectively. NBO results indicate a charge transfer of 0.092 |e| from the N atom of nicotine to the B atom of the nano-cage. Conversely, for physisorption, the distance between carbon atoms on the nicotine ring and B atoms of the nano-cage ring ranges from about 3.43 to 3.49 Å. A less negative E_b (-8.16 kcal/mol) suggests weak physical adsorption of nicotine on the nano-cage due to Van der Waals

forces. Hence, the N atom of nicotine emerges as the thermodynamically more favorable site for adsorption on the B atoms of the nano-cage. This insight directs subsequent investigations to focus solely on the interaction of the N atom of nicotine with nano-cage structures. Notably, the electronic properties of the $B_{12}N_{12}$ nano-cage undergo significant variation upon nicotine chemisorption, as indicated by the calculated DOS plots (Figure 3), showing a decrease in E_g value from 9.34 eV in the pristine nano-cage to 7.84 eV after nicotine chemisorption (approximately 16.05% change). This underscores the sensitivity of the $B_{12}N_{12}$ nano-cage's electronic properties to the presence of the nicotine molecule. Collectively, these findings suggest strong adsorption of nicotine on the $B_{12}N_{12}$ nano-cage, positioning the nano-cage as a promising candidate for nicotine adsorption. Further investigation into the solvation properties of the chemisorption configuration was pursued for a comprehensive understanding of nicotine adsorption.

Figure 1

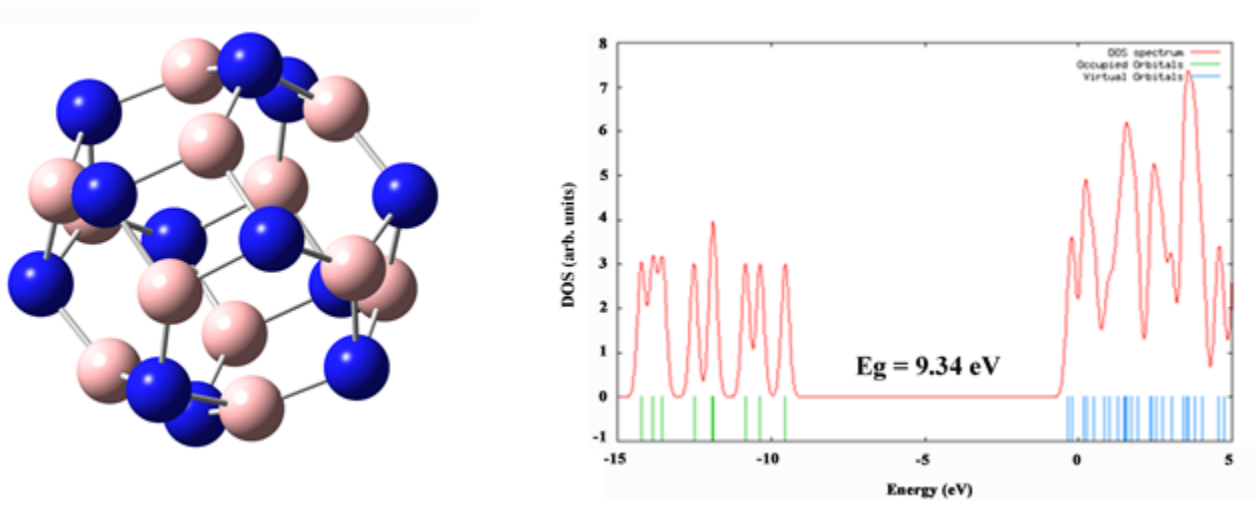

Fig. 1. The optimized structure of $B_{12}N_{12}$ nano-cage and its density of states (DOSs).

Solvation energies (E_{solv}):

The solvation study focused solely on pristine $B_{12}N_{12}$ and configuration A, the most stable form, optimizing their structures in both gaseous and aqueous phases. Solvation energies (E_{solv}) were calculated as 4.38 kcal/mol and 13.42 kcal/mol for pristine and configuration A, respectively, indicating higher water solubility for configuration A.

An essential property for characterizing structure and reactivity is the electric dipole moment (DM).[28] Configuration A exhibited a significant increase in DM from 0.00 Debye in the pristine nano-cage to 7.82 Debye. This increase primarily contributes to the enhanced solubility. In the solvent phase, the dipole moment rose to 10.61 Debye for configuration A due to electron polarization from solvation. Additionally, the E_{ad} increased from -37.65 kcal/mol to -43.75 kcal/mol in the solvent phase, suggesting an increase in nicotine molecule electron donation with a polar solvent present.[29]

Exploring the impact of structural variations in $B_{12}N_{12}$ on nicotine adsorption compared to its pure form, we introduced doping. Firstly, aluminum (Al) and phosphorus (P) dopants replaced boron and nitrogen atoms, respectively. Al doping increased the distance between N and Al atoms to 1.97 A°, with a band gap variation of 10%. Interaction with adjacent B atoms resulted in a band length of 1.64 A°, and a negligible change in electronic properties. Conversely, chemisorption behavior of nicotine on the P-doped nano-cage surface showed only weak van der Waals interactions, with the lowest Eb (-7.53 kCal/mol) compared to other systems investigated. The DOS plot revealed a 7.89% band gap variation between $B_{11}PN_{12}$ in the presence and absence of nicotine.[30]

Fig. 2. Computed electrostatic potentials on the molecular surfaces of a single Nicotine molecule. The surfaces are defined by the 0.0004 electrons/b3 contour of the electronic density. Color ranges, in a.u.: blue, more positive than 0.010; green, between 0.010 and 0; yellow, between 0 and -0.010; red, more negative than -0.010. (For interpretation of the references to color in this figure legend, the reader is referred to the web version of this article.)

Figure 2

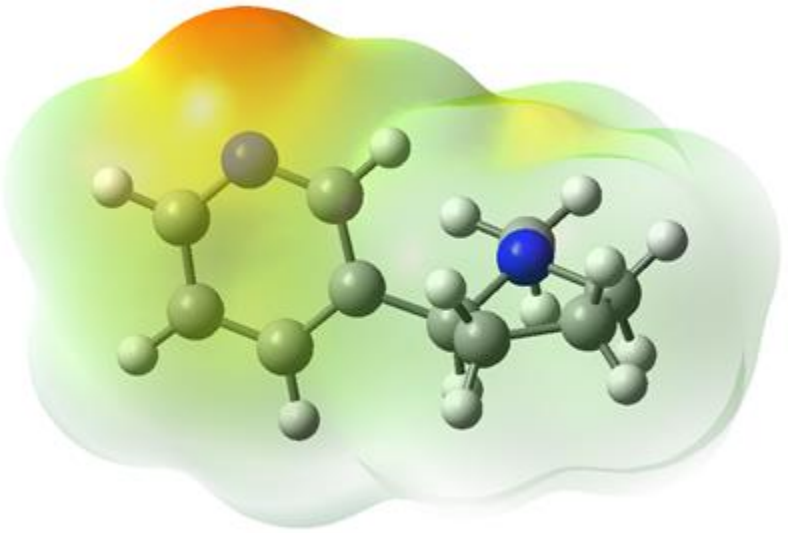

Fig. 3. Models for two stable A: chemisorption and B: physisorption configurations and their density of states (DOSs) plots. Distances are in A°.

Figure 3

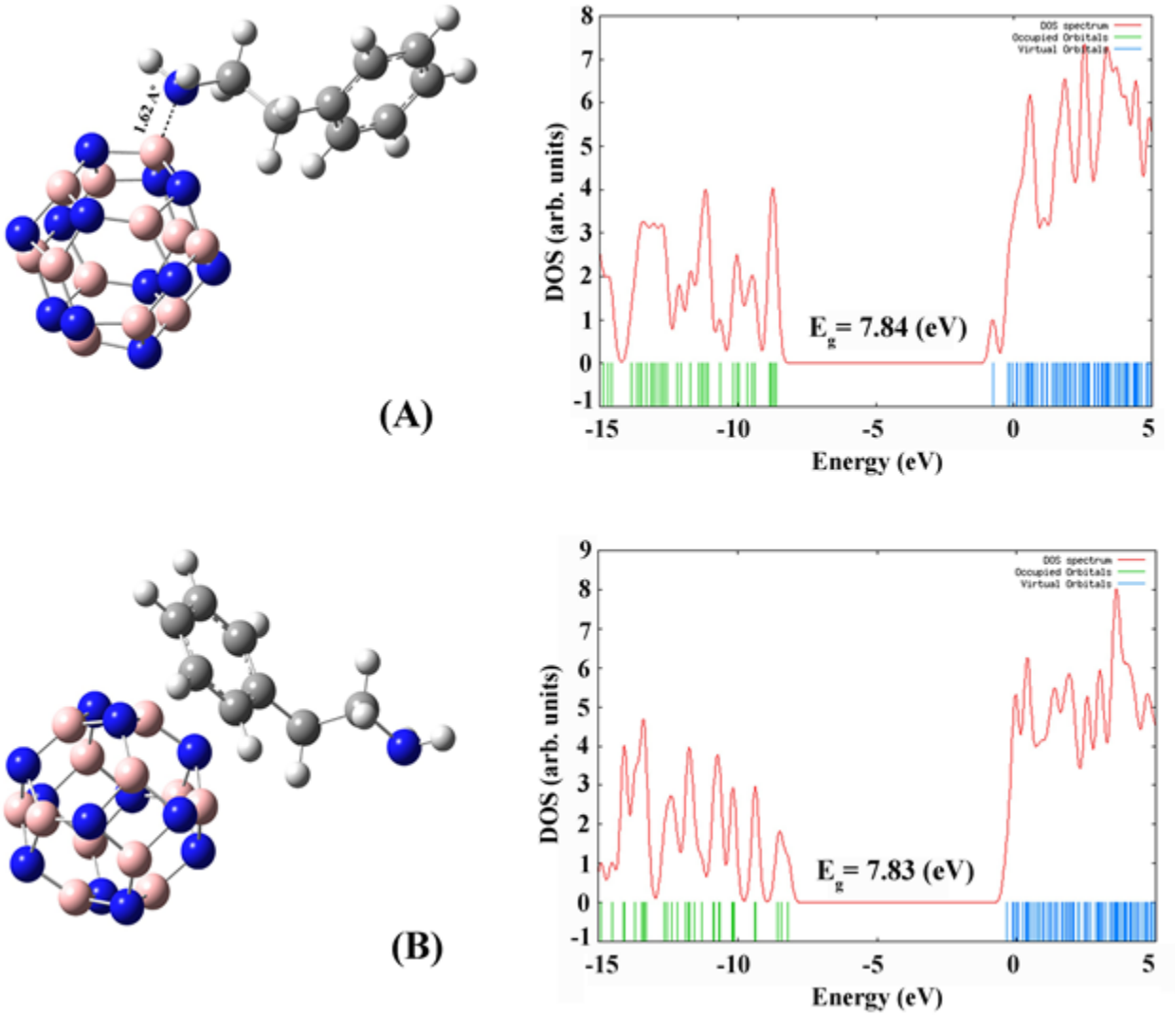

To analyze the characteristics of bond critical points (BCP) at different interaction sites of nicotine on pristine, P- and Al-doped $B_{12}N_{12}$ complexes, Bader theory has been applied. In the equilibrium geometrical condition, an interatomic interaction line is regarded as a bond path. Molecular graphs of the mentioned complexes are depicted in Fig. 5. For N-B, N-Al, H-N and H-P interactions, there are corresponding bond paths and critical points (BCPs) within the

equilibrium structures. As indicated in previous studies, the characteristics of donor-acceptor BCPs are very useful to obtain a profound perception of the nature of interactions. Parameters such as electron density at the donor-acceptor BCP (ρc) its Laplacian ($\nabla.\nabla$ ρc)often correlate with the bond energy or other parameters like donor-acceptor distance and etc. According to Table 2, two bond paths are observed in the $B_{12}N_{12}$-Nicotine complex. The calculated electron densities at N-B and H-N bond critical points are found to be about 0.124 and 0.010 a.u respectively. These values proved that the most stable configuration is obtained when NIC interacts from its N site with the B site of $B_{12}N_{12}$.

The calculated electron density properties of the $B_{12}N_{12}$-Nicotine demonstrate that N-B bonding has high ρ, and positive value (0.291). These properties are typical of closed-shell interactions and clarify electrostatic features of the N-B bonding. According to the literature, positive values of and HC indicate an electrostatic nature for interaction whereas a partially covalent nature is expected for interaction when is positive and HC has a negative value [31]. HC is the electron energy density at BCP which is equal to the sum of kinetic electron energy density (KC) and potential electron energy density (VC).[31]

In the case of $B_{11}AlN_{12}$, it seems that the most stable configuration belongs to the one that Nicotine interacts from its N site with the Al site of $B_{11}AlN_{12}$. According to the results, N-Al has a partial covalent nature and it can be concluded that the value of electron density in N-Al BCP decreases in comparison with N-B interaction in $B_{12}N_{12}$-Nicotine complex.

For instance, the average value of (0.124 a.u.) for the N-B bond in B12N12-NIC is approximately 94% more than the one in B11AlN12-NIC complex (0.064 a.u.).

In the case of $B_{12}N_{11}P$-Nicotine, according to the Fig. 5C, four bond paths have been detected in AIM plot. Analyzing of one of these paths (H…. P) shows that the interaction has low ρ (0.006

a.u.), positive value (0.018) and negative HC. These properties are typical of partial covalent interactions. Finally, it is obvious that the capacity of the nano-cages to concentrate electrons at the BCP is sensitive to the interaction sites.

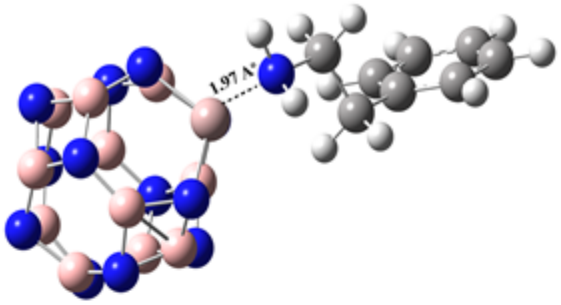

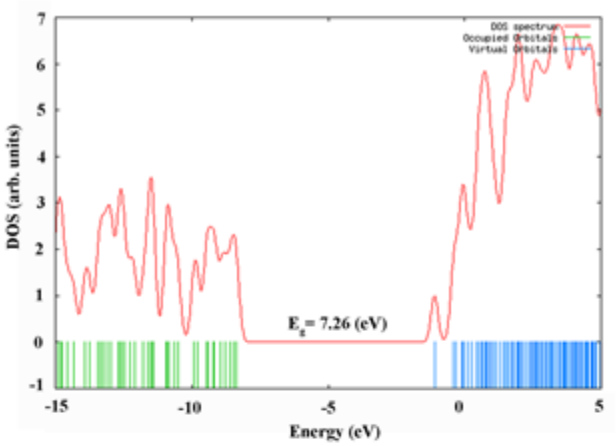

(A)

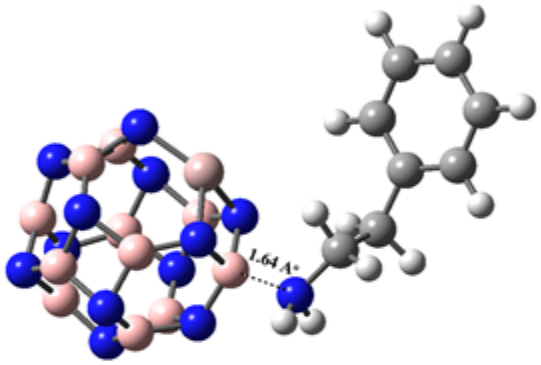

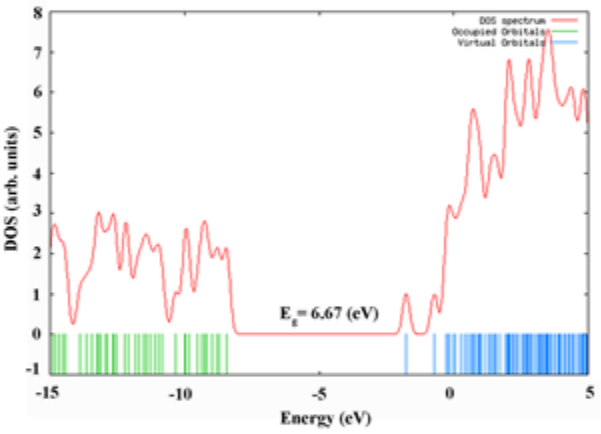

(B)

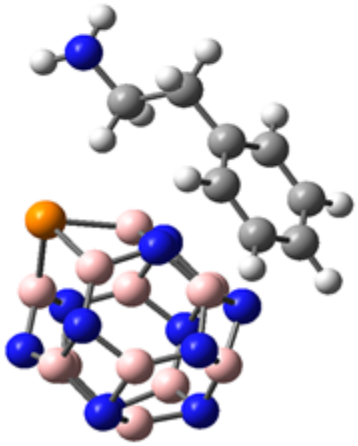

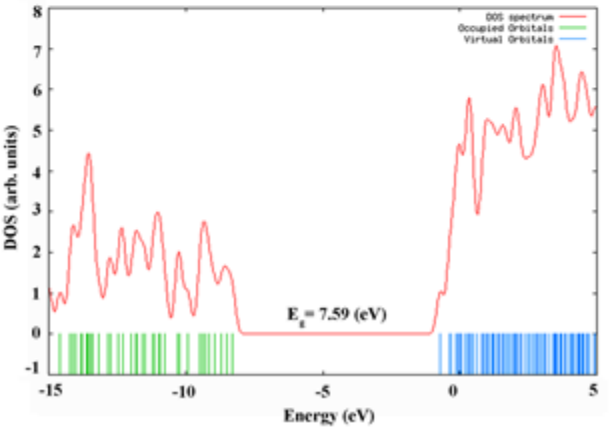

(C)

Fig. 4. Models for $B_{11}AlN_{12}$-Nicotine stable chemisorptions in two configurations A: N-Al and B: N-B interactions, C: $B_{12}N_{11}P$-NIC and their density of state (DOS) plots. Distances are in A0.

Figure 5

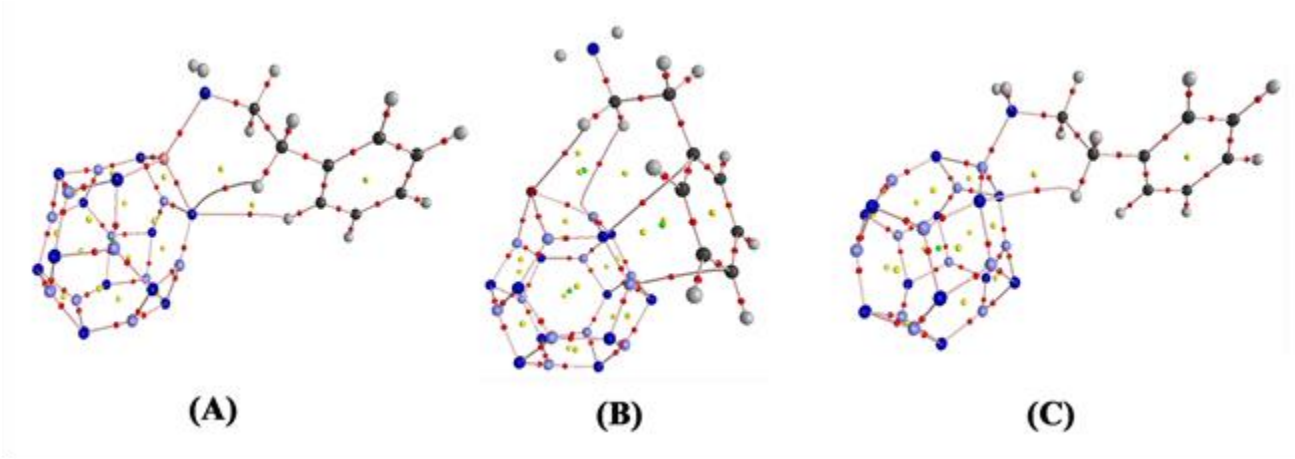

Fig. 5. Molecular graph of A: $B_{12}N_{12}$-Nicotine, B: $B_{11}AlN_{12}$-Nicotine and C: $B_{12}N_{11}P$-Nicotine complexes. The graphs were obtained at the M06/6–311++G** level. Large circles correspond to attractors and small red (dark grey in print) and yellow (light grey) circles are bond and ring critical points, respectively.The lines are bond paths.

Table1. Energy of Adsorption (E_b) (kcal/mol), HOMO-LUMO Energies and HOMO-LUMO Gaps (E_g) (eV), Bond Distance (Å), at M062x/6-311++G.**

Structure	L(A^0)	E_{tot} (a.u)	E_b (Kcal/mol) BSSE (cor)	HOMO(eV)	LUMO(eV)	E_g (eV)	ΔE_g %	μD
$B_{12}N_{12}$	-	-	-	-9.54	-0.20	9.34	-	0.00
$B_{12}N_{12}$-Nic(Config1)	1.61	-1455.09	-37.38	-8.39	-1.55	6.84	27	11.40
$B_{12}N_{12}$-Nic(Config2)	1.61	-1455.09	-37.75	-8.39	-1.55	6.84	27	11.40
$B_{12}N_{12}$-Nic(Config3)	-	-1455.04	-3.82	-7.85	-0.47	7.38	21	2.88
$B_{12}N_{12}$-Nic(Config4)	-	-1455.04	-4.36	-7.82	-0.51	7.31	22	3.25

Conclusion:

This study investigates the adsorption of Nicotine on $B_{12}N_{12}$ nano-cage and its Al- and P-doped derivatives using density functional calculations. Results indicate that Nicotine prefers adsorption on the B site of pristine $B_{12}N_{12}$ and $B_{12}N_{11}P$, with adsorption energies of approximately -37.65 and -7.53 kcal/mol, respectively. Adsorption alters the HOMO and LUMO energy levels and E_g of both pristine and doped $B_{12}N_{12}$ derivatives, suggesting $B_{12}N_{12}$ as a potential Nicotine sensor. Additionally, solvation effects were examined, revealing that a polar solvent enhances Nicotine adsorption on the $B_{12}N_{12}$ surface. AIM calculations suggest an electrostatic nature for N-B interaction in Nicotine-$B_{12}N_{12}$ and partial covalent for N-Al in

Nicotine-$B_{11}Al$-N_{12}. These findings contribute to understanding $B_{12}N_{12}$ and its doped derivatives as effective adsorbents for Nicotine, shedding light on common interactions within $B_{12}N_{12}$ nano-cages.

References:

1. Waldum, H.L., et al., *Long-term effects of inhaled nicotine.* Life sciences, 1996. **58**(16): p. 1339-1346.
2. Rezvani, A.H. and E.D. Levin, *Cognitive effects of nicotine.* Biological psychiatry, 2001. **49**(3): p. 258-267.
3. Mishra, A., et al., *Harmful effects of nicotine.* Indian Journal of Medical and Paediatric Oncology, 2015. **36**(01): p. 24-31.
4. Heishma, S.J., R.C. Taylor, and J.E. Henningfield, *Nicotine and smoking: a review of effects on human performance.* Experimental and Clinical Psychopharmacology, 1994. **2**(4): p. 345.
5. Ernst, M., et al., *Smoking history and nicotine effects on cognitive performance.* Neuropsychopharmacology, 2001. **25**(3): p. 313-319.
6. Dwyer, J.B., S.C. McQuown, and F.M. Leslie, *The dynamic effects of nicotine on the developing brain.* Pharmacology & therapeutics, 2009. **122**(2): p. 125-139.
7. Oku, T., et al., *Synthesis, atomic structures and properties of carbon and boron nitride fullerene materials.* Materials Science and Engineering: B, 2000. **74**(1-3): p. 206-217.
8. Oku, T., et al., *Formation, atomic structures and properties of boron nitride and carbon nanocage fullerene materials.* International Journal of Inorganic Materials, 2001. **3**(7): p. 597-612.
9. Padash, R., M.R. Esfahani, and A.S. Rad, *The computational quantum mechanical study of sulfamide drug adsorption onto X12Y12 fullerene-like nanocages: detailed DFT and QTAIM investigations.* Journal of Biomolecular Structure and Dynamics, 2021. **39**(15): p. 5427-5437.
10. Yu, X., et al., *Recent advances and remaining challenges of nanostructured materials for hydrogen storage applications.* Progress in Materials Science, 2017. **88**: p. 1-48.
11. Sun, X., et al., *Amantadine antiparkinsonian drug adsorption on the AlN and BN nanoclusters: A computational study.* Physics Letters A, 2020. **384**(5): p. 126128.
12. Xu, S.-h., et al., *Stability and property of planar (BN) x clusters.* Chemical physics letters, 2006. **423**(1-3): p. 212-214.

13. Oku, T., A. Nishiwaki, and I. Narita, *Formation and atomic structure of B12N12 nanocage clusters studied by mass spectrometry and cluster calculation.* Science and Technology of Advanced Materials, 2004. **5**(5-6): p. 635-638.
14. Ejiofor, E.U., et al., *Exploring the potential of single-metals (Cu, Ni, Zn) decorated Al12N12 nanostructures as sensors for flutamide anticancer drug.* Heliyon, 2023. **9**(10).
15. Ghasemi, A., et al., *Adsorption behavior of metformin drug on boron nitride fullerenes: Thermodynamics and DFT studies.* Journal of Molecular Liquids, 2019. **275**: p. 955-967.
16. Ghasemi, A.S., et al., *A study on the effect of 1-butyl-4-methylpyridinium bromide adsorption on the structural and electronic properties of B12N12 nano-cage.* Journal of Molecular Liquids, 2019. **277**: p. 115-122.
17. Javan, M.B., et al., *Interaction of B12N12 nano-cage with cysteine through various functionalities: a DFT study.* Superlattices and Microstructures, 2016. **100**: p. 24-37.
18. Saadh, M.J., et al., *Inhibitory effects of menthol, B12N12, B16N16, Al12N12, Al16N16, and their complexes on tumor necrosis factor-alpha (TNF-α) and their potential anti-inflammatory activity: A study using DFT and molecular docking.* Inorganic Chemistry Communications, 2024: p. 112187.
19. Soltani, A., et al., *Serine adsorption through different functionalities on the B12N12 and Pt-B12N12 nanocages.* Materials Science and Engineering: C, 2018. **92**: p. 216-227.
20. Schmidt, M.W., et al., *General atomic and molecular electronic structure system.* Journal of computational chemistry, 1993. **14**(11): p. 1347-1363.
21. Zhao, Y. and D.G. Truhlar, *The M06 suite of density functionals for main group thermochemistry, thermochemical kinetics, noncovalent interactions, excited states, and transition elements: two new functionals and systematic testing of four M06-class functionals and 12 other functionals.* Theoretical chemistry accounts, 2008. **120**: p. 215-241.
22. Hehre, W.J., R. Ditchfield, and J.A. Pople, *Self—consistent molecular orbital methods. XII. Further extensions of Gaussian—type basis sets for use in molecular orbital studies of organic molecules.* The Journal of Chemical Physics, 1972. **56**(5): p. 2257-2261.
23. Keith, T.A., *AIMAll (Version 14.11. 23).* TK Gristmill Software: Overland Park, KS, USA, 2014.
24. Miertuš, S., E. Scrocco, and J. Tomasi, *Electrostatic interaction of a solute with a continuum. A direct utilizaion of AB initio molecular potentials for the prevision of solvent effects.* Chemical Physics, 1981. **55**(1): p. 117-129.
25. Bahrami, A., et al., *A first-principles study on the adsorption behavior of amphetamine on pristine, P-and Al-doped B12N12 nano-cages.* Superlattices and Microstructures, 2013. **64**: p. 265-273.
26. Heidar-Zadeh, F., et al., *Information-theoretic approaches to atoms-in-molecules: Hirshfeld family of partitioning schemes.* The Journal of Physical Chemistry A, 2017. **122**(17): p. 4219-4245.
27. Popelier, P., *Quantum molecular similarity. 1. BCP space.* The Journal of Physical Chemistry A, 1999. **103**(15): p. 2883-2890.
28. Foresman, J. and E. Frish, *Exploring chemistry.* Gaussian Inc., Pittsburg, USA, 1996. **21**.
29. Biegler-Konig, F., J. Schonbohm, and D. Bayles, *Software news and updates-AIM2000-A program to analyze and visualize atoms in molecules*. 2001, John Wiley & Sons Inc 605 THIRD AVE, NEW YORK, NY 10158-0012 USA. p. 545-559.

30. Lewars, E.G., *Computational chemistry*. Introduction to the theory and applications of molecular and quantum mechanics, 2011. **318**.
31. Keith, T., R. Bader, and Y. Aray, *Structural homeomorphism between the electron density and the virial field*. International journal of quantum chemistry, 1996. **57**(2): p. 183-198.